Localized exciton bound to an isoelectronic trap in silicon

J. Weber, W. Schmid, and R. Sauer
Physikalisches Institut (Teil 4) der Universität Stuttgart, Pfaffenwaldring 57, D-7000 Stuttgart 80, Federal Republic of Germany
(Received 20 August 1979)

A photo- and electroluminescence study is reported on the recombination radiation from excitons bound to an isoelectronic trap in silicon. This type of luminescence is novel in silicon. The luminescence which was obtained from only few samples consists of three long-lived emission lines A, B, and C, and a number of associated weak phonon wings. The decay characteristics and the temperature dependence of the fluorescence along with the "forbidden" B line exhibited under perturbations of a magnetic or elastic strain field give rise to our interpretation in terms of an isoelectronic trap binding the electron-hole pair. These features are highly reminiscent of familiar isoelectronic systems which can bind an exciton such as GaP:N, GaP:Bi, or ZnTe:O. Orientational Zeeman measurements show that the trap has axial symmetry in the $\langle 111 \rangle$ direction. The g factors are $g_e = 1.6 \pm 0.1$ and $g_h = 1.1 \pm 0.1$. The g_e value is largely reduced in comparison with known bound-electron values and suggests that an electron is tightly bound to the trap capturing the hole by its Coulomb field. This conception also explains the observed cw-excitation dependence of the fluorescence. The samples showing the A, B, and C fluorescence are n and p type ($\rho \geq 2$ Ω cm) and are grown by different techniques. The strongest fluorescence is observed from an aluminum-doped sample (2.5 Ω cm) for which the trap density is estimated to be no more than some 10^{13} cm^{-3}. No correlation of luminescence with shallow-donor or -acceptor doping could be established, and the nature of the trap remains unidentified. A correlation of luminescence with carbon concentration in a number of samples and the annealing behavior of the exciton luminescence may hint that carbon is one of the trap constituents.

I. INTRODUCTION

Recombination radiation from excitons bound to isoelectronic traps in semiconductors is known since 1962. ZnTe:O is the earliest example where Dietz *et al.*[1] first observed the new type of fluorescence, and Hopfield *et al.*[2] in 1966 identified oxygen to be the trap which binds the exciton. Similarly, Thomas *et al.*[3] and Yafet and Thomas[4] in 1963 demonstrated the existence of an electron-hole pair bound to a "spinless" impurity in GaP, and Thomas *et al.*[5,6] in 1966 identified this center as nitrogen. Other isoelectronic traps which bind excitons were then discovered such as Bi in GaP by Trumbore *et al.*[7] which was extensively studied in succeeding works,[8-11] Te in CdS by Aten *et al.*,[12,13] and Bi in InP by Dean *et al.*[14] with extended investigations in recent years.[15,16] These traps are point defects substituting for a host atom on a lattice site. Studies on further isoelectronic point defects binding an exciton were reported, e.g., Sn in Ge,[17] but are less well authenticated. More complex compound centers were also found to act as isoelectronic traps in GaP. These are ZnO or CdO pairs substituting for Ga or P, respectively, on nearest-neighbor lattice sites.[18,19] Dean[20] reported a triple isoelectronic trap Li-Li-O of C_{3v} axial symmetry in GaP were O and one Li impurity replace a nearest-neighbor pair of P and Ga, respectively, and the remaining Li atom occupies an interstitial lattice site on this $\langle 111 \rangle$ axis.

A survey on isoelectronic impurities was given by Czaja,[21] and more recently, Dean[22] and Baldereschi[23] reviewed isoelectronic traps both experimentally and theoretically.

In the present paper, we report a new isoelectronic system in silicon. In nine silicon samples we detect three novel emission lines. In view of the obvious analogy in many features to familiar isoelectronic exciton luminescence, e.g., to that in GaP:N, these lines are labeled A and B with a third extra line named C. These lines are different from the P, Q, and R lines which were recently studied by Mitchard *et al.*[24] in In-doped Si and were attributed to isoelectronic centers involving In and possibly carbon or oxygen. The A, B, C exciton emission is strong in no-phonon (NP) luminescence. Weak phonon replicas are observed both in photoluminescence and in electroluminescence. The phonon structure, however, is more clearly seen in electroluminescence since the strong superposed free-exciton (FE) TO-phonon assisted radiation is quenched in the latter excitation mode. The NP luminescence determines the exciton binding energy with respect to the excitonic gap to be ≈33 meV. Luminescent intensities of the dominant A line are most prominent between 10 and 20 K, the absolute intensities vary from sample to sample by factors of up to ≈20. Temperature- and excitation-dependent measurements and the decay kinetics show that A, B, and C excitons belong to an exciton system in different J-J-coupled states

(for brevity we shall use A, B, C for the emission lines as well as for the exciton states). In the B exciton, the bound exciton and the bound hole form a $J=2$ state, and transitions to the crystal ground state, $J=0$ are dipole forbidden, but become allowed when the B state is perturbed by external fields. In the A state, electron and hole momenta are coupled to $J=1$, and the A line is predominant under most experimental conditions. C is an excited exciton state split by ≈ 3 meV. The measured decay times are temperature dependent, and the A and B exciton lifetimes derived from an analysis of the experimental data are extremely long, $\tau_A = 2.2$ μsec and $\tau_B = 1.1$ msec. This gives evidence that the exciton is bound to an isoelectronic trap. Zeeman measurements yield g factors $g_e = 1.6$ and $g_h = 1.1$ which suggest that the electron is tightly bound capturing a hole by its Coulomb field. Consistency with this model is obtained from a rate-equation analysis of the experimental excitation dependence which shows a characteristic change in the observed power-law dependence from exponent 1 to ≈ 0.5 at relatively small excitation levels. Orientational Zeeman measurements reveal the $\langle 111 \rangle$ symmetry of the isoelectronic trap, so that the correct classification of the A and B exciton states is $J_z = \pm 1$ or $J_z = \pm 2$ rather than $J=1$ and $J=2$, respectively. C is then most probably correlated with the excited states $|J, J_z\rangle = |1,0\rangle$, $|1,\pm 1\rangle$, and $|2,0\rangle$. Absorption of the A, B, C lines could not be detected. Instead, even at small intensities of the incandescent lamp used *luminescence* was observed due to the high radiative quantum efficiency of the exciton recombination. Comparison of Al-bound exciton (A^0X) absorption in the "best" sample Si:Al (2.5 Ω cm) determines an upper bound to the density of the isoelectronic traps of some 10^{13} cm^{-3}.

The samples were immersed in liquid helium in conventional Dewars. A special cryostat was employed in the temperature-dependent measurements constructed after the suggestion of Gmelin[25] and operated with liquid helium as a coolant. This cryostat was designed to maintain adjustably a constant temperature between ≈ 1.5 and ≈ 60 K at relative high excitation levels up to 50 mW. Green argon-ion or red krypton-ion laser lines, $\lambda = 514$ nm and $P \leq 2$ W or $\lambda = 647$ nm and $P \leq 500$ mW, respectively, were used for cw excitation of the spectra. Time-resolved experiments were performed by GaAs laser-array pulse excitation. The spectra were dispersed by $\frac{3}{4}$-m or 1-m Spex grating monochromators, photoelectrically detected either by a cooled S-1 cathode photomultiplier or by a cooled PbS cell, and processed by lock-in technique or by gated photon counter technique.

The paper is organized in the following way: First, we give the basic spectra and describe the temperature dependence and the decay kinetics of the lines. These data were briefly reported elsewhere[26] and led to the interpretation of an isoelectronic binding center. We then report new results on Zeeman measurements which reveal the axial nature of the center, and on the excitation level dependence of the A line. Electroluminescence is reported which reveals the phonon structure of the bound transitions free from FE radiation. To our knowledge, this is the first efficient sharp-line injection luminescence in silicon. Annealing data are described at the end, and the possible nature of the trap is discussed. Most results refer to Si:Al (2.5 Ω cm) as our standard material since the A, B, C lines are most strongly observed in this particular crystal, but equivalent data were obtained from all specimens which showed the novel luminescence.

II. EXPERIMENTAL RESULTS AND DISCUSSION

A. Spectra due to the localized exciton

Figure 1 represents two spectra taken with a sample of Al-doped Si of size $1 \times 2 \times 8$ mm immersed in liquid helium. The spectrum at low excitation level in Fig. 1(a) shows a recombination radiation due to Al bound excitons (A^0X) in the $J=0$ and $J=2$ hole states as NP-, TA-, and TO-phonon assisted luminescence. The low-energy sideband of the A^0X lines is the m_2 multiple bound exciton radiation.[27,28] The A line is seen at $\lambda = 1.1044$ μm at an intensity comparable to that of the A^0X line. For small size samples, the intensity ratio I_A/I_{A^0X} depends sensitively on the excitation density since the samples are heated above the 4.2-K bath temperature. This yields an easy method of observing the novel fluorescence unless temperature constancy is required. At increased excitation densities, line A grows immensely but a new satellite line C split by 3.1 meV comes up even more rapidly [Fig. 1(b)]. Simultaneously, the A^0X doublet line is quenched with a strongly enhanced intensity ratio of the $J=2$ to the $J=0$ line components. On the basis of the Vouk and Lightowlers work on acceptor bound exciton luminescence,[29] this ratio may serve as an accurate calibration of temperature in Al-doped Si which is particularly useful in the low-temperature regime. We shall demonstrate in Sec. II B that in the high-temperature regime up to ≈ 30 K the C/A intensity ratio is itself a convenient index of temperature.

The positions of the A and C lines are sensitive neither to the doping donor or acceptor species nor to the doping level. At elevated temperatures,

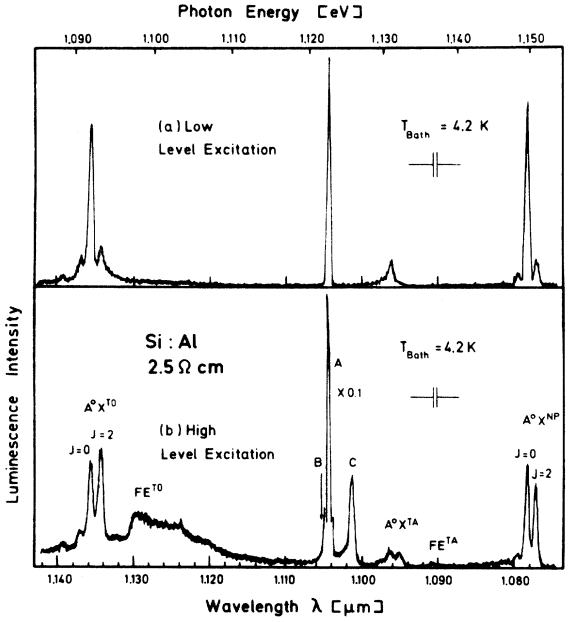

FIG. 1. Luminescence from A and B excitons in a sample of Si:Al (2.5 Ω cm) at two temperatures generated by different laser-induced sample heating. The spectra are photoelectrically recorded with a S-1 cathode photomultiplier and are not corrected for the wavelength-dependent sensitivity of the detector. (a) The excitation corresponds to a pump power of less than 100 mW illuminating a sample spot of ≈ 1-mm diameter; (b) the excitation corresponds to ≈ 400-mW laser power focused to a much smaller spot than in (a). The crystal temperature in (b) is $T \approx 12$ K. The line positions are $\lambda(A) = 1.1044$ μm and $\lambda(C) = 1.1014$ μm.

line A shifts to lower energies, its position at 35 K is about 0.4 meV below the low-temperature position. This effect is due to band-gap shrinkage. With the band-gap energy $E_g(T) = a + bT + cT^2$ and the parameters $a = 1.170$ eV, $b = 1.059 \times 10^{-5}$ eV/K, and $c = -6.05 \times 10^{-7}$ eV/K^2 according to Bludau *et al.*,[30] we obtain $\Delta E_g(35\text{ K}, 4.2\text{ K}) = -0.40$ meV in agreement with the observed A-line shift. At low temperatures, line A is very sharp with half-width $\Delta h\nu \leq 0.01$ meV but broadens upon temperature increase above ≈20 K. Line C is always much broader with a typical width of ≈0.75 meV. It is asymmetric exhibiting a low energy tail, but does not indicate substructure as to several superposed close falling lines (see Fig. 1 of Ref. 26). In Sec. II F it is shown that the A line at $\lambda = 1.044$ μm is a NP transition. Taking the excitonic gap as $E_{gx} = 1.1552$ eV, we find the A-exciton localization energy $E_{Bx}(A) = 32.6$ meV. This binding energy is much larger than for all excitons localized at familiar donors or acceptors except for Tl ($E_{Bx} = 44.8$ meV)[31].

B. Temperature dependence

The A- and C-line intensities were quantitatively studied as a function of temperature (Fig. 2). The C/A intensity ratio corresponds to a Boltzmann factor $\exp(\Delta/kT)$. Hence, the A- and C-exciton states are in thermal equilibrium. The activation energy $\Delta = -3.2 \pm 0.1$ meV is in excellent agreement with the spectroscopic A to C line spacing of 3.1 meV. The same exponential temperature dependence of the C/A intensity ratio as drawn in Fig. 2 for Si:Al was found for another two samples investigated. In contrast to this common feature the *absolute* A-line intensities are not generally identical under temperature variation. Results for two samples are plotted in Fig. 2. In the low- and the high-temperature regimes, the dependence was found to be identical for all samples but in the intermediate temperature range it varies from sample to sample. At low temperatures, there is an activation of line A by $\Delta \approx -1$ meV, at high temperatures line A is quenched with a quenching activation energy of 44 ± 2 meV. The initial activation is suggestive of a third exciton state B below the A level which does not radiate but acts as a thermal supply to A upon increased temperature. The existence of the B state is confirmed by kinetic and Zeeman measurements (Secs. II C and II D). The intermediate temperature range is not understood because it is intricate and differs for different samples. The observed thermal behavior may be due to several cooperating supply and exhaustion channels, e.g., the supply of charge carriers from thermally quenched shallow donor or acceptor bound excitons D^0X or A^0X, respectively, or by D^- or A^+ centers. All these complexes have binding energies ≈2–5 meV (D^- and A^+)[32-34] or ≈4–5 meV (D^0X, A^0X)[35] suitable to account for such processes. The luminescence maximum of the A

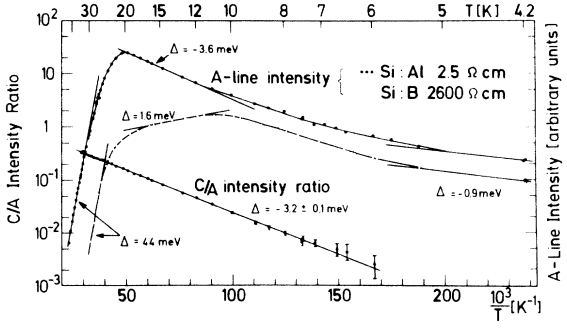

FIG. 2. Temperature dependence of the A-line intensity in two different samples (right scale) and intensity ratio of C to A lines (left scale). The thermal quenching energy of the A line, $\Delta = 44 \pm 2$ meV, and the thermal activation energy of C from A, $\Delta = -3.2 \pm 0.1$ meV, were obtained from least-squares fits.

line at $T = 18-20$ K was not only observed for Si:Al but also for some P-doped samples. We do not know, however, in how far this behavior is typical of P or Al doping, or how specific the break is for B doping at T = 11 K. These questions are open at the present time.

There is a discrepancy between the spectroscopically determined localization energy $E_{Bx}(A) = 32.6$ meV and the thermal activation energy $\Delta(A) = 44 \pm 2$ meV. The former energy, however, should be augmented by the FE binding energy, $E_{FE} = 14.7$ meV,[36] in order to come to the total binding energy of the A exciton with respect to the band gap $E_{tot}(A) = 47.3$ meV. Similar but much heavier discrepancies between E_{tot} and $\Delta < E_{tot}$ were observed in the case of the isoelectronic impurity Bi in GaP by Trumbore *et al.*[7] and for the yet unknown isoelectronic center involving In in Si as recently described by Mitchard *et al.*[24] Trumbore *et al.* originally gave an explanation of this effect by assuming that only one of the mobile particles is thermally released, whereas the difference of E_{tot} and Δ is due to the particle that remains at the center. In the present case, we may argue that the observed activation energy is approximately equal to the total binding energy; the remaining slight discrepancy may then originate from the experimental uncertainty of Δ and from the fact that the asymptotic slope of the curve defining Δ has not yet experimentally been reached in the high temperature regime in Fig. 2.

A smaller activation energy which would correspond to the thermal release of one particle from the excitonic complex is not unambiguously visible in Fig. 2. However, this dissociation mechanism may be partly compensated by the earlier mentioned supply processes. In the net result, this may lead to the intermediate weak intensity decrease of the A line which is in Fig. 2 observed ($\Delta = 1.6$ meV) for the low-doped Si:B sample.

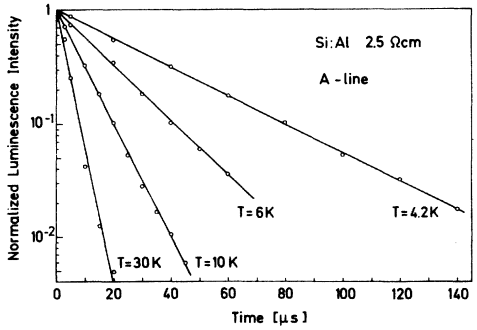

FIG. 3. A-line luminescent intensities for various temperatures vs time. The excitation source is a GaAs laser-array of pulse width 2 μsec. The number of data points in the figure is reduced; depending on temperature up to 30 points were actually measured for one temperature.

C. Decay kinetics

Figure 3 is a plot of A-line luminescent intensities versus time after excitation by a pulsed GaAs laser at various temperatures. The decay is exponential in each case over the entire range of fluorescent intensities which in some measurements were observed over more than three decades. From about 8 K on the C line is also strong enough to be accurately measured. Whenever under the same experimental conditions the A line as well as the C line could be observed, their decay was identical. This is an independent proof of the thermal equilibrium between the A- and C-exciton states. From these measurements we deduce the decay time-versus-temperature plot which is reproduced in Fig. 4. In Fig. 4 there is a strong characteristic variation of decay times with temperature. It is obvious from a comparison with Fig. 2 that the striking high-temperature decrease ($T \geq 20$ K) is due to the dissociation of the exciton. At low temperatures, we obtain extremely long decay times approaching 1 msec, but even the extrapolated high temperature limit, $\tau \approx 4.5$ μsec, is large when compared with familiar lifetimes of shallow donor or acceptor bound excitons. For D^0X or A^0X excitons, the lifetimes strongly depend on the exciton binding energy E_{Bx}, or by virtue of the Haynes rule, on the impurity binding energy E_i. Experimentally, approximate dependencies $\tau \propto E_i^{-3.9}$ for donors or $\tau \propto E_i^{-4.6}$ for

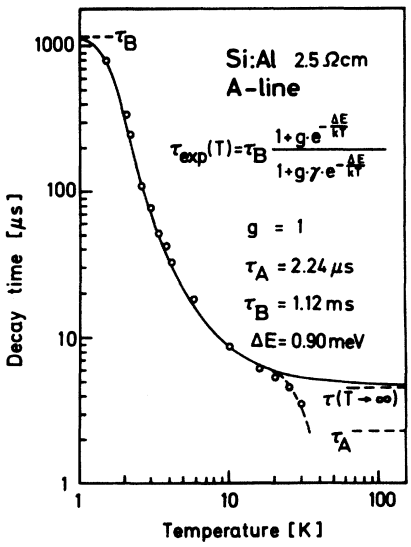

FIG. 4. Variation of A-exciton decay times with temperature (circles are experimental). The variation is analogous to fluorescent exciton decay times in the isoelectronic systems GaP:N, GaP:Bi, and ZnTe:O as measured by Cuthbert and Thomas (Ref. 37). The fit (full line) is represented by the inserted formula with parameters $\tau_A = 2.24$ μsec, $\tau_B = 1.12$ msec, and $\Delta E = 0.90$ meV.

acceptors were reported,[37] and were interpreted by a localized phononless Auger recombination process.[37-39] For example, excitons are localized at In acceptors in silicon with $E_{Bx}=13.7$ meV and they decay rapidly with $\tau=2.7$ nsec.[37] Our present exciton binds more strongly by a factor of ≈ 2.5 but nevertheless decays more slowly by a factor $>10^3$ even at high temperatures. These dramatic discrepancies give evidence that an electron and a hole constitute the A, B, and C excitons and that a third mobile particle which would bring about short Auger determined lifetimes is not involved. Thus, the exciton is bound to a center acting as an isoelectronic trap.

An electron with spin-$\frac{1}{2}$ and a Γ_8 hole with $j=\frac{3}{2}$ may couple to form two exciton states with the total momentum $J=1$ or $J=2$. We anticipate the results obtained in Sec. IID which show that the exciton is bound to an axial center of C_{3v} symmetry. The correct classification of the low lying exciton states is then $J_Z=\pm 1$ or $J_Z=\pm 2$ where J_Z denotes the component along the $\langle 111\rangle$ axis of the center. We associate the strong A line with dipole allowed transitions from the $J_Z=\pm 1$ exciton state to the $J=0$ crystal ground state. The $J_Z=\pm 2$ state is expected to lie below the $J_Z=\pm 1$ state since electron and hole charges have different signs. Transitions from the $J_Z=\pm 2$ state are dipole forbidden. We explain the observed temperature dependence of the decay times by thermal population of the radiating $J_Z=\pm 1(A)$ state from the low-lying nonradiating $J_Z=\pm 2(B)$ state where A and B states have different lifetimes τ_A or τ_B, respectively. Under these assumptions, an expression

$$\tau_{expt}(T)=\tau_B\frac{1+g\exp(-\Delta E/kT)}{1+g\gamma\exp(-\Delta E/kT)} \quad (1)$$

is derived.[40] Here $\gamma=\tau_B/\tau_A, g=1$ is the ratio of degeneracy of the $J_Z=\pm 1$ and $J_Z=\pm 2$ exciton states, and ΔE denotes the A to B level splitting. This expression was used to fit the experimental points $\tau_{expt}(T)$ in Fig. 4. This procedure fixes values of τ_B and ΔE in fairly narrow limits while larger scope is allowed for the value of τ_A. A good fit is obtained with $\tau_A=2.24$ μsec, $\tau_B=1.12$ msec, and $\Delta E=0.90$ meV. The latter value is consistent with but more reliable than the thermal value which may be read from Fig. 2.

The exceptionally large lifetime τ_B of the B exciton which we obtain from this analysis leads us to conclude that the radiative quantum efficiency of the exciton is close to unity. The lack of a B-exciton transition in the spectra suggests that the dipole selection rule is strongly fulfilled. If a small portion of B excitons would recombine radiatively the associated luminescence intensity would have to be smaller than the A line intensity by a factor $>10^3$ or we would have detected the B line. Hence, we conclude that τ_B is essentially determined by nonradiative recombination. Assuming further that the A exciton has a nonradiative lifetime comparable to that of the B exciton so that $\tau_A\approx\tau_{rad}$, we find from the familiar relationship $\eta=\tau_{nonrad}(\tau_{rad}+\tau_{nonrad})^{-1}$ a radiative quantum efficiency η of about unity.

D. Zeeman measurements

Zeeman measurements were performed with a superconducting magnet up to 5.3 T in Voigt configuration. Figure 5(a) shows a Zeeman spectrum for $\vec{H}\,||\,[110]$ and Fig. 5(b) depicts the positions of the observed line components as a function of magnetic field strength H. The three high-energy components belong to the A transition and can be observed at all field strengths. The three lower components are due to the B transition and show up only for fields exceeding ≈ 1.5 T growing upon increased magnetic fields. The B components split linearly with H and can be extrapolated to zero field with high accuracy. This determines the B exciton level at an energy 0.90 meV below the A exciton level consistent with the thermal and kinetic values.

In Fig. 5(c), the integrated luminescence intensity of all B-exciton associated components I_B to the integrated luminescence of all A-exciton as-

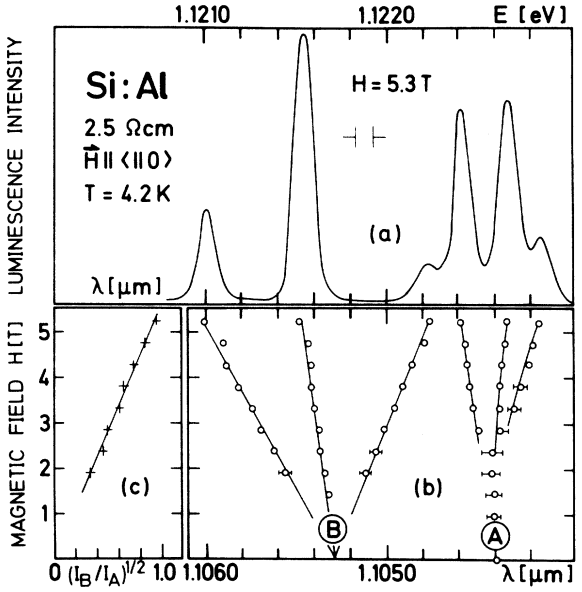

FIG. 5. (a) Zeeman spectrum for the maximum field strength, $H=5.3$ T, and for $\vec{H}\,||\,[110]$ in Voigt configuration. The lines observed are unpolarized; (b) splitting of A and B transitions as a function of magnetic field strength H for $\vec{H}\,||\,[110]$; (c) ratio of integral luminescence from B and A lines, I_B/I_A, vs magnetic field strength for $\vec{H}\,||\,[110]$. A straight line corresponding to $I_B/I_A\propto H^2$ interconnects the data points.

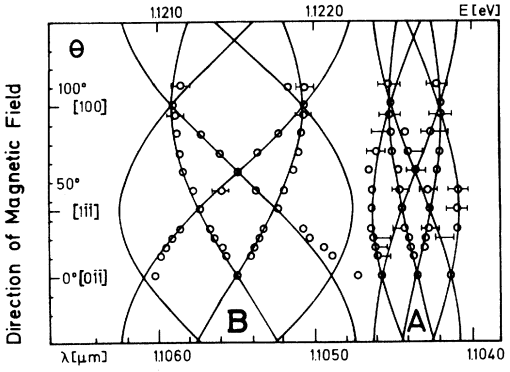

FIG. 6. Splitting of A and B transitions vs direction of $\vec{H}$ at $H=5.3$ T as $\vec{H}$ was rotated in a plane perpendicular to the $[0\bar{1}1]$ direction. θ is the angle between the $[0\bar{1}\bar{1}]$ crystal direction and the magnetic field $\vec{H}$. Full lines are fits using Eqs. (2) with $g_e=1.6$ and $g_h=1.1$.

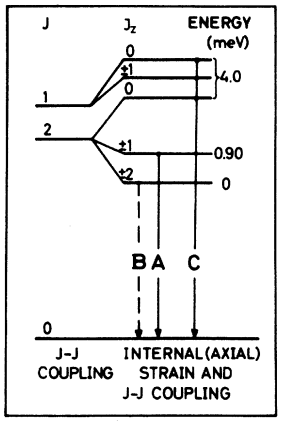

FIG. 7. Exciton states as formed by J-J coupling of a spin-$\frac{1}{2}$ electron and a Γ_8, $j=\frac{3}{2}$ hole, and related dipole transitions to the $J=0$ ground state. Left-hand side: Exciton in T_d symmetry of a point defect with no cubic crystal field splitting of the $J=2$ level. Right-hand side: Exciton in an axial field of C_{3v} symmetry, J_Z is the component of J along the axial crystal field (Ref. 41). Energies are experimental, the exciton structure is almost quantitatively identical with that of excitons bound to isoelectronic Li-Li-O traps in GaP (Ref. 20).

sociated components I_A is plotted versus the magnetic field strength, and a quadratic dependence $I_B/I_A \propto H^2$ is obtained. The splitting of the A and B lines is strongly anisotropic as revealed by orientational measurements which are illustrated in Fig. 6. The splittings of the A and B lines as a function of field orientation relative to the crystal axes are reminiscent of the isoelectronic systems GaP:CdO (Ref. 19) and GaP:Li-Li-O (Ref. 20) suggesting an axial symmetry of the present exciton trap. From Fig. 6 we expect the center axis to be aligned along the $\langle 111\rangle$ direction because the smallest number of Zeeman components is seen for $\vec{H}$ parallel to a [100] direction when all [111] axes are equivalent. On this basis we closely follow the argumentation of Henry *et al.*[19] in their discussion of isoelectronic CdO traps in GaP. Introduction of the axial center reduces the cubic T_d symmetry to C_{3v} and removes the fourfold degeneracy of the $j=\frac{3}{2}$ hole. The total angular momentum of the exciton, $J=1$ or $J=2$, is no longer a good quantum number. The exciton states have to be requantized along the [111] axis of the center, and the Z component of the angular momentum, J_Z, remains a constant of motion where Z is defined along the [111] center axis. The four hole states split into two Kramers doublets $j_Z=\pm\frac{3}{2}$ and $j_Z=\pm\frac{1}{2}$, the electron states are $j_Z=\pm\frac{1}{2}$. The electron states and the $j_Z=\pm\frac{3}{2}$ hole states form four low-lying exciton states, two with $J_Z=\pm1$ and two with $J_Z=\pm2$. The $J_Z=\pm1$ level gives rise to the dipole allowed A line, transitions from level $J_Z=\pm2$ corresponding to the B-exciton state are forbidden. Higher energy exciton states with $J_Z=0$ and $J_Z=\pm1$ are made up from hole states $j_Z=\pm\frac{1}{2}$ and the electron states $j_Z=\pm\frac{1}{2}$. The relations between the exciton states obtained from J-J coupling and those in a field of C_{3v} symmetry are shown in Fig. 7 after Morgan and Morgan.[41] If the hole and electron states are split in a magnetic field as $\pm\frac{3}{2}g_h\mu_B H_Z$ or $\pm\frac{1}{2}g_e\mu_B H_Z$, respectively, the four lower exciton states will have energies

$$E_A=\pm(\tfrac{3}{2}g_h-\tfrac{1}{2}g_e)\mu_B H_Z\,,$$
$$E_B=\pm(\tfrac{3}{2}g_h+\tfrac{1}{2}g_e)\mu_B H_Z\,, \qquad (2)$$

where H_Z is the magnetic field component along the center axis. These formulas imply that A and B lines split into identical patterns but that the magnitude of the splitting corresponds to the sum or to the difference of the electron and hole g factors, respectively. This expectation is verified by the experimental splittings in Fig. 6. The full lines in Fig. 6 are fits to the data points on the basis of the above formulas where E_A and E_B have been adjusted to the A and B line splittings for $\vec{H}\parallel[111]$. There is excellent agreement between theory and the complete set of experimental data except for a significant discrepancy at small angles $\theta\approx0°$ which arises for the higher-energy B component and might be due to interactions of this component with the closely positioned low-energy A component. From the fits we obtain

$$g_e=1.6\pm0.1,\quad g_h=1.1\pm0.1\,.$$

The value of g_h is consistent with g factors found for shallow acceptor bound holes but the electronic g value is smaller than the values obtained for shallow donor or D^0X bound electrons. From the

work of Feher *et al.*[42] on EPR, we extract hole values $g_1'(\mathrm{B}) = 1.21$, $g_1'(\mathrm{Al}) = 1.19$, $g_1'(\mathrm{Ga}) = 1.14$, and $g_1'(\mathrm{In}) = 1.00$ where the anisotropic contributions to the g factors, g_2', increase with acceptor binding energy but are small compared to g_1' even for In with $g_2' = -0.08$.[43] Hence, g_1' virtually correlates with g_h. For donor-bound electrons, g_e(Sb) = 1.998 58 was reported by Feher[44] with a donor specific reduction by some 10^{-4} with increasing binding energy, visualized $g_e(\mathrm{P}) = 1.998\,50$ and $g_e(\mathrm{As}) = 1.998\,37$. The electronic g value of As bound excitons was obtained by Cherlow *et al.*[45] from the Zeeman splitting of the D^0X luminescence to be $g_e = 1.85$, and is corroborated by unpublished work of two of the authors on P bound exciton Zeeman spectroscopy yielding $g_e = 1.87$.[46] These data show that the magnitude of g_e depends on the nature of the electron state. Our present value $g_e = 1.6$ is significantly smaller than all familiar electron g factors. It may be concluded that in the A-, B-exciton system the electron is first captured and tightly bound to the isoelectronic axial center by a short-range potential, and that the hole is bound by this Coulombic acceptor-like field. Assuming the alternative case of initial hole capture followed by Coulombic donorlike binding of the electron we would expect the g_e value to be close to that of shallow donor electrons rather than so small as observed.

Henry *et al.*[19] pointed out that a component of the magnetic field perpendicular to the ⟨111⟩ symmetry axis will not split the exciton states but will mix them making transitions from B exciton states observable when the magnetic field is present. They derived a ratio of the B to the A transition rates

$$W_B/W_A = I_B/I_A = (g_e\mu_B H_\perp/\Delta E)^2, \qquad (3)$$

where $\Delta E = E_A - E_B$ at zero field. This expression explains why we were not able to detect the outer B-line components (Fig. 6). These are split by the maximum amount, equivalent with the highest H_Z so that $H_\perp$ is small resulting in a negligible admixture of A-exciton states.

On the basis of the A- and B-line Zeeman measurements, it is believed that line C arises from transitions between the excited $J_Z = 0, \pm 1$ exciton states and the crystal ground state (Fig. 7). With respect to this extra C line, our spectra are most reminiscent of spectra in the GaP:Li-Li-O isoelectronic system where two high-energy lines appear in excess of the $J_Z = \pm 1$ and $J_Z = \pm 2$ lines.[20] Deviating from this case our C line is single and there is no indication of a substructure. Zeeman measurements could give answer as to the precise origin of this line; however, hitherto we could not perform such experiments with the superconducting magnet since thermal occupation of the C-exciton level is too low for $T \leq 8$ K. Current experiments with samples as small as possible aim to make the C line sufficiently strong for high resolution luminescence measurements by sample heating at 4.2-K bath temperature. It was initially pointed out (see Fig. 1) that this method is successfully applicable to the exciton system.

Piezospectroscopy has also been performed on a number of samples. Uniaxial stress applied along the principal crystal directions induces fluorescence from B components in addition to A components. The B components can be detected for stress magnitudes $\gtrsim 150 \times 10^5$ N/m^2 = 150 kbar Extrapolation of the B component positions to zero stress results in an A- to B-line separation of 0.9 meV consistent with the previous data. A detailed study of A and B piezospectroscopy will be given in a separate paper. As to the C line, we encounter similar difficulties as in the Zeeman measurements. Work on stress-dependent C line luminescence in a variable-temperature Gmelin-type cryostat equipped with a stress supply is in progress.

E. cw-excitation dependence

The excitation dependence of the A line was examined at 4.2 K for two samples but with preference to Si:Al. These measurements were performed under krypton and argon laser pumping with relatively large size samples to prevent heating of the crystals. Relying on the A^0X, $J = 2$ to $J = 0$ luminescence ratio as a sensitive probe of constant temperature, we applied the maximum unfocused laser output power without detectable temperature increase beyond 4.2 K. Results on Al doped Si are plotted in Fig. 8. The acceptor bound exciton A^0X, $J = 0$ luminescence is exactly

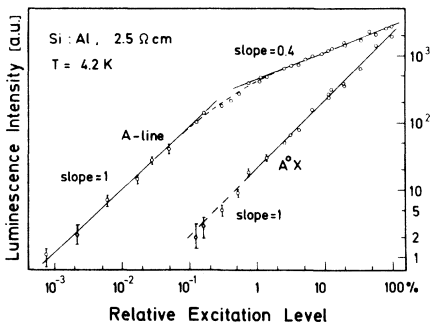

FIG. 8. Dependence of A exciton and Al-bound exciton radiation on cw-excitation level. 100% excitation corresponds to 500-mW laser power entering the optical cryostat and illuminating a sample spot of ≈ 1-mm diameter. Temperature was constant as probed by the A^0X, $J = 2$ to $J = 0$ exciton luminescence ratio.

linear as a function of excitation level throughout the hole range of pump levels. The A line, however, shows a characteristic change from a linear dependence at low excitation levels to an almost square root dependence at high levels. Such characteristic behavior was observed in several independent measurements on Si:Al and on a strongly radiating Si:P (115 Ω cm) sample (see Table I) and yielded low-level slopes of 1 and high level slopes of 0.43 and 0.45. Higher-temperature experiments at 20 K were also simultaneously performed on the A and C lines. We found a constant C to A intensity ratio throughout the range of excitation levels, and a knee separating low and high excitation regimes with slopes of unity or ≈0.5, respectively.

It is the latter square root dependence of the A-line intensities on higher excitation levels which is not a common feature of bound-exciton (BE) luminescence and, therefore, requires a special explanation. We consider the A^0X excitation dependence first. Assuming that free excitons FE are primarily formed which are then localized at Al acceptors a linear dependence of A^0X luminescence on excitation is expected as experimentally obtained. In principle, saturation effects might occur because the number of impurities available to bind excitons is limited. Such effects were actually observed in Si:B (600 Ω cm or $\approx 2\times10^{13}$ cm^{-3}) or in Si:P (100 Ω cm or $\approx 5\times10^{13}$ cm^{-3}).[48,49] B acceptors are particularly suitable for bound exciton saturation due to their large bound exciton decay time $\tau_{BE}\approx 1$ μsec.[37,48] In the present case, saturation need not be considered since the Al doping is on order 2.5 Ω cm or $\approx10^{15}$ cm^{-3}, and the A^0X decay time, $\tau_{BE}=76$ nsec,[37] is much shorter than for B or P bound excitons. No saturation of the A^0X luminescence was in fact observed for any experimental condition in the present experiments.

In contrast, saturation effects *should* occur for the A exciton because the decay time is exceptionally large, $\tau_A=30$ μsec (4.2 K), and the trap density is low, $N_t\lesssim 10^{13}$ cm^{-3}, as estimated in Sec. II G. Complete saturation would yield a horizontal line in Fig. 8 which could experimentally not be obtained. We explain the square root dependence in Fig. 8 as the result of "partial" saturation. We consider the formation of the A, B, C excitons as a two-step process where an electron is captured first by the isoelectronic trap to form an intermediate negatively charged trap state which then attracts a hole. These processes may be characterized by two formation times which inversely depend on the capture probabilities of electrons or holes, respectively, to their associated trap states, and the number densities of these trap states. A quantitative analysis of these processes was made in terms of reaction kinetic rate equations for the case that simultaneously acceptor (or donor) bound excitons form via FE capture, and assuming homogeneous excitation of the sample. For the sake of brevity, we outline merely two results. At low excitation levels, the total formation time is short since there are enough traps available to capture electrons and holes. In this case, the number density of isoelectronic excitons N_x is governed by the exciton decay time τ_A. This results in a linear pump power dependence

TABLE I. Samples containing the isoelectronic trap. Indicated are the room-temperature resistivities and the growth technique (FZ float zone, Cz Czochralski material). The carbon concentrations were obtained from ir vibrational band absorption. Oxygen concentrations marked by bars are below the detection limit (5×10^{15} cm^{-3}) for vibrational ir absorption, the oxygen concentrations which are indicated for B- and Al-doped samples were determined from tunneling spectroscopy (Ref. 47); this method yields a detection limit of $<5\times10^{14}$ cm^{-3}.

Sample doping	ρ (Ω cm)	Growth technique	C (cm^{-3})	O (cm^{-3})	A-line luminescence
P	10	FZ	$\geq3\times10^{17}$	——	moderately strong
P	12	FZ	$\geq2\times10^{16}$	——	weak
P	33	FZ	1.4×10^{16}	——	very weak
P	115	FZ	4×10^{16}	——	strong
P	200	FZ	7×10^{16}	——	weak
Sb	4	Cz		$\approx10^{17}$	weak
B	2600	FZ		$\leq5\times10^{14}$	strong
Al	2.5	FZ	3×10^{18}	$\approx10^{15}$	very strong
Au(Al)	150(p type)	FZ		$\leq10^{16}$	weak

$$N_x = \tau_A g , \tag{4}$$

where g is the generation rate. At higher excitation levels, the total formation time may become much larger than τ_A since the number densities of trap states available for the capture processes saturate. In this case, N_x is governed by the slower or the two capture processes which depends on the electron or hole density alone. This is in contrast to the acceptor bound exciton A^0X where FE capture is assumed and, hence, the product of electron and hole densities enters into the capture rate.

The A^0X recombination channel predominates the A-, B-, C-exciton recombination channel; first because the trap density N_t is small compared to the acceptor concentration (see Sec. IIG), second because the A-exciton decay, $\tau_A = 30$ μsec, is very much larger than the A^0X decay time, $\tau_{BE} = 76$ nsec. Thus, we may assume approximately equal number densities of electrons and holes. Based on these assumptions, we find for the high excitation regime the expression

$$N_x = N_t \beta (g/\alpha_0)^{1/2} / [1/\tau_x + \beta (g/\alpha_0)^{1/2}] , \tag{5}$$

where β is composed of electron and hole capture probabilities to the trap states and α_0 is the capture probability of electrons and holes in the FE formation process from free carriers. Equation (5) describes a square root dependence of N_x on the excitation level which eventually saturates as expected.

F. Electroluminescence

An important point is the detection that the A and C lines can easily be electrically excited. A sample of our standard material, Si:Al (2.5 Ω cm) of size $1 \times 2 \times 8$ mm was etched ($2\,HNO_3 + 1\,HF + 2\,CH_3COOH$), and a film of high-purity gold of thickness ≈0.1 μm was evaporated on the two large opposite areas. This device was an Ohmic resistance at room temperature. At liquid-nitrogen temperature the current-voltage characteristic completely changed to a symmetric diode characteristic, and upon further temperature lowering remained virtually the same, as is represented for T = 4.2 K in Fig. 9. Exciton radiation from one of the 1×8 mm areas perpendicular to the gold-deposited areas was observable in the current range from 0.01 to 50 mA. In this range the luminescence intensities increased exponentially with slope ≈0.8 (Fig. 9) except for a short steeper increase at 10 mA succeeded by a very rapid drop. From about 3 mA on the C line was also observed coming up in relation to the A line upon increasing currents. The absolute intensities of A and C lines are comparable with the intensities at photoexcitation when $U \times I$ is on order of the laser excitation power. A number of selected spectra are shown on the left side of Fig. 9. The current dependence of the C/A luminescence ratio suggests an effective sample heating when the currents are increased. Hence, the intensity-to-current relation in Fig. 9 is probably due to the combined effects of excitation and temperature enhancement where the excitation effect alone would contribute a slope 0.4–0.5 (Fig. 8). It may be concluded that a large voltage drop across the non-Ohmic contacts dissipates most electric power in a small region of the device; otherwise injection excitation in the large sample volume of ≈16 mm^3 would not produce temperatures higher than the bath temperature since even the small-volume photoexcitation on the same order in Fig. 8 has no effect on temperature. Future experiments are aimed to produce low-temperature low-resistivity Ohmic contacts for even more efficient injection excitation.

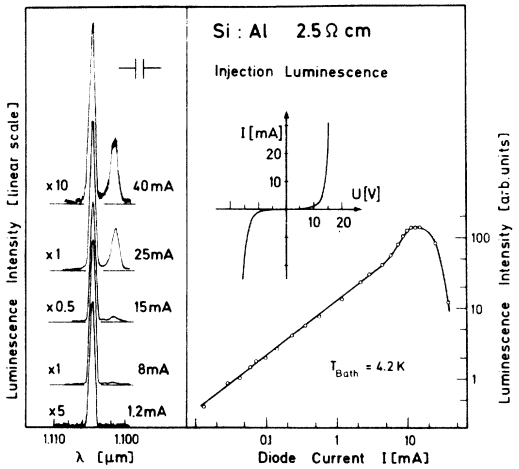

FIG. 9. Electroluminescence in Si:Al. Left-hand side: Original spectra at various currents showing A and C lines. Right-hand side: Intensity-vs-current relation and the I-U characteristic of the device employed. Sample geometry is 1×2×8 mm.

Injection luminescence turned out to be helpful in determining the phonon assisted spectrum of the A and C lines. In Fig. 10 we compare the low-energy spectra obtained by injection or photoexcitation and for approximately equal temperatures. The main difference between these spectra is the absence of FE luminescence in the electrically excited spectrum. Taking the C/A luminescence ratio as a probe of temperature we estimate from Fig. 2 that T ≈ 18 K. In photoexcited n- or p-type samples, FE radiation is by far the strongest luminescence at such temperatures. At currents below 5 mA the FE luminescence was not seen at

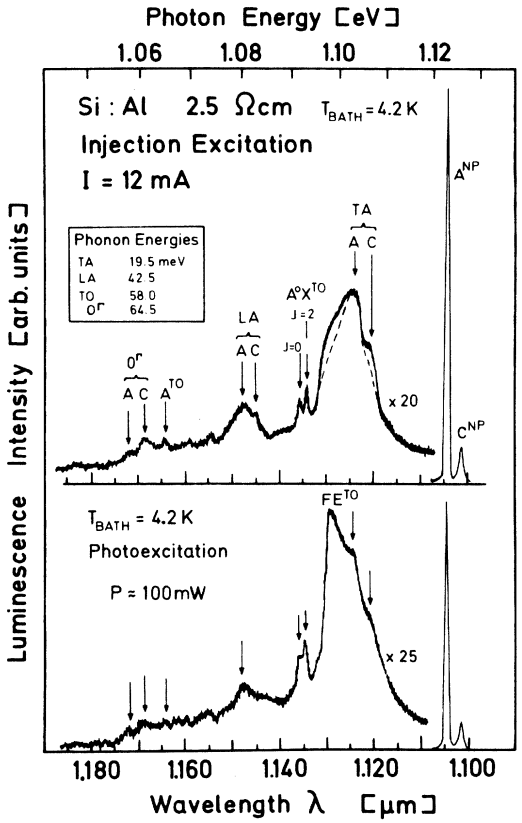

FIG. 10. Luminescence spectra due to injection and photoexcitation. Top: Excitation current $I = 12$ mA, applied voltage $U \approx 14$ V (Fig. 9); the dashed line indicates the form of the spectrum at low currents. The hump at $\lambda = 1.130$ μm is due to remaining FE radiation. Bottom: Laser power 100 mW on ≈ 1 mm^2 sample spot. The crystal temperature is approximately the same in both spectra, the vertical intensity scales are identical.

all. At higher currents a relatively weak remainder could be detected which does not essentially disturb the A- and C-line spectra and was found to slightly increase when the current was increased. It is probable that the free excitons are quenched by impact ionization but this point needs further investigation. The absence of free excitons enabled us to detect the TA-phonon assisted C- and A-line replicas which are usually obscured by the FE luminescence (compare Fig. 1). Except for two narrow lines due to TO-phonon transitions from the $J = 0$ and $J = 2$ hole states of the Al-bound exciton there are a number of broad phonon sidebands associated with the A and C lines. Although it is difficult to analyze the bands due to their weakness and large width, some of them unambiguously reveal a doublet structure with a line separation of ≈ 3 meV. We attribute these doublet lines to A- and C-exciton radiation with the participation of TA, LA, and O(Γ) phonons. The TO-phonon assisted A line is also seen but it can not be decided from the available spectra whether there is an associated TO-phonon sideband of C. It is remarkable that the TA-phonon energy derived from our spectra is slightly larger than the energies which are familiar from high-accuracy low-temperature D^0X or A^0X luminescence.

These phonon energies compare with the present values from Fig. 10 as follows:

Phonon	A, C luminescence (meV)	D^0X, A^0X luminescence (meV)
TA	19.5 ± 0.2	18.7
LA	42.5 ± 0.2	...
TO	58.0 ± 0.2	58.1
O(Γ)	64.5 ± 0.2	64.5 (Ref. 50)

The LA-phonon energy is consistent with the phonon dispersion curves from inelastic neutron scattering.[51] LA-phonon participation is not known for D^0X, A^0X, or FE radiative recombination. All samples showed comparable relative oscillator strength in the phonon wings. This is different from GaP:N where Thomas and Hopfield[6] pointed out that the intensity ratio of the NP to the phonon lines can differ largely from sample to sample.

The analysis of the phonon wings in Fig. 10 defines the lines at 1.1044 and 1.1014 μm as NP transitions and thus determines the excitonic binding energy $E_{Bx} = 32.6$ meV (A line) which was initially reported.

G. Absorption measurements

Absorption measurements on the A, B, C lines were performed but with negative results. Preliminary measurements on thin samples were repeated with samples of increasing thickness, and finally, a specimen of 6 cm relevant transmission length was employed. "White" light from in incandescent lamp was passed through a Jarrel-Ash 0.25-m Ebert monochromator which at widely opened slits operated as a variable band filter synchronized with the absorption spectrometer. Even at low intensities of the illuminating light as usually employed for absorption measurements, we observed the A line in *luminescence*. We ascribe this effect to the very high radiative quantum efficiency of the A-exciton recombination and to a low trap density N_t, and estimate an upper bound of N_t. We use Dexter's formula[52] on impurity absorption

$$N_t = 9.6 \times 10^{15}\ \text{cm}^{-3}[n/f_A(\alpha_{max}\Gamma)]\,, \qquad (6)$$

where n is the refractive index, f_A represents the oscillator strength of the A line, and $(\alpha_{max}\Gamma)$ re-

places the integral absorption $\int \alpha d\nu$ assuming Gaussian line broadening. The oscillator strength is given by

$$f_A = \left(\frac{1.45\lambda^2}{n\tau_A}\right)\left(\frac{g_i}{g_f}\right). \quad (7)$$

Here λ is the transition wavelength (in cm), τ_A is the lifetime of A excitons; g_i, g_f are the degeneracies of the initial and final states, and an effective electron mass of $m^* = 0.322 m_0$ was taken which accounts for the prefactor. Inserting $\lambda = 1.1044 \times 10^{-4}$ cm, $n = 3.4$, $\tau_A = 2.2$ μsec, $g_i = 1$, and $g_f = 2$ we obtain $f_A = 1.2 \times 10^{-3}$. Combination of this value with Eq. (6) yields

$$N_t = 2.7 \times 10^{19}\ \text{cm}^{-3}\ [(\alpha_{\max}\Gamma)_A], \quad (8)$$

where $(\alpha_{\max}\Gamma)_A$ denotes the total absorption of the A line with the inclusion of all phonon replicas. The ratio of absorption of the no-phonon A line to the total absorption may be estimated from the corresponding areas under the fluorescence spectrum. For this estimate, a 5-mA electroluminescence spectrum was used showing no FE luminescence. After a correction for the photomultiplier sensitivity which strongly drops towards longer wavelengths we find as an approximate ratio

$$(\alpha_{\max}\Gamma)_A / (\alpha_{\max}\Gamma)_{A^{NP}} = \int_A I\, d\nu \Big/ \int_{A^{NP}} I\, d\nu \approx 3.5, \quad (9)$$

which yields

$$N_t = 9.5 \times 10^{19}\,\text{cm}^{-3}[(\alpha_{\max}\Gamma)_{A^{NP}}]. \quad (10)$$

Actually, there is no absorption of the A exciton in the best sample, Si:Al (2.5 Ω cm). Hence, we apply the same consideration as above to the bound exciton absorption $(A^0X)^{TO}$, which was recorded in all trial experiments on the A-exciton absorption, and estimate the smallest detectable value of $(\alpha_{\max}\Gamma)_{A^{NP}}$ from a comparison with the A^0X absorption. For Al, we may use the doping level $N_d(\text{Al}) \approx 5 \times 10^{15}$ cm^{-3} and the oscillator strength $f_{\text{Al TO}} = 2.9 \times 10^{-5}$ from Ref. 53 as given parameters yielding

$$(\alpha_{\max}\Gamma)_{\text{Al TO}} = N_d f_{\text{Al TO}}/9.6 \times 10^{15}\ \text{cm}^{-3} n = 4.4 \times 10^{-6}. \quad (11)$$

Our most sensitive spectra were recorded using derivative techniques. The A-exciton absorption would still be detectable if it were weaker than the $(A^0X)^{TO}$ absorption by a factor of at least 10, most probably even by a factor of 50. The former ample value results in the upper bound for the trap density

$$N_t \leq 9.5 \times 10^{19}\ \text{cm}^{-3} \times 4.4 \times 10^{-7} = 4.2 \times 10^{13}\ \text{cm}^{-3}. \quad (12)$$

This is the maximum concentration arrived at for the Al-doped sample. All other specimens show the A, B, C lines weaker (see Table I) so that trap concentrations are assumed to be no larger than $\approx 10^{12}$ cm^{-3} for most of the samples.

H. Nature of the trap

Table I is a compilation of all samples showing A, B, C luminescence along with a characterization of the material. There is no obvious and striking feature which distinguishes these samples from others which do not exhibit the novel luminescence. The nine samples in Table I were obtained from trial experiments performed on more than 60 specimens in the doping range up to some 10^{16} cm^{-3} which were either on hand or were specifically selected under the aspect of high carbon concentration. The isoelectronic trap is found to exist in n- and p-type material doped with different shallow donors or acceptors. Low-temperature high-resolution spectroscopy on the luminescence from D^0X or A^0X complexes proves that all samples in Table I are essentially uncompensated with negligible codoping. Even in the 2600-Ω cm high-resistivity B-doped sample BE luminescence due to contamination of P is hardly observable. These circumstances in combination with the insensitivity of the A, B, C line positions on donor or acceptor species give evidence that the trap is not formed by nearest-neighbor pairs of substitutional donors or acceptors, as is the case in GaP with Cd_{Ga}-O_P pairs. The A, B, C luminescence appears to be absolutely incorrelated with shallow donors or acceptors. This excludes also vacancy-impurity clusters which exist in several configurations in Si.[54] The trap is present in pulled (Czochralski-grown, Cz) silicon as well as in float zone (FZ) material. There is, however, only one suitable Cz-grown sample doped with Sb, and hence, no conclusions can be drawn at the present time as to correlations between the trap and growth technique. Such investigations are highly desirable.

In our brief communication on the A, B, C excitons[26] we suggested that carbon may be involved in the trap. We arrived at this conclusion because in the early experiments on the first four samples (Al-doped and three P-doped crystals listed at the top of Table I, there was an evident correlation of exciton luminescence with carbon concentration. It has now turned out that this correlation is not as general as initially believed (see Table I). The Zeeman experiments showed the axial nature of the center which must, therefore, consist of at least two constituents which are not both carbon since in this case a prevailing correlation with

carbon concentration would be expected. A new hint to carbon playing a role in the formation of the trap may come from recent isochronal anneal experiments. The luminescence from A excitons was investigated after the samples had been subjected to a 1-h anneal under Ar buffer gas at several temperatures between room temperature and 1000 °C. The results of independent recordings obtained at different days and under moderately distinguished experimental conditions are shown in Fig. 11. The ratios of A-line intensity to A^0X line intensity are drawn on the coordinate. These ratios are thought to be an adequate measure of what occurs to the A, B, C excitons: For the temperatures applied, Al should not be largely influenced and hence, the A^0X line intensities should not much vary with temperature; this was actually observed in the majority of the measurements. On the other hand, taking the intensity ratios removes the effects of accidental absolute intensity changes due to different optical alignments during the independent runs. We find that the A-exciton fluorescence is quenched at about 200 °C, but comes up once more at higher temperatures up to 400 °C before it finally vanishes. Such intricate annealing behavior is not unfamiliar and was often observed for lower-energy sharp emission lines due to the recombination of electrons and holes at defect centers introduced into silicon by radiation damage.[55] It is tempting to correlate the annealing behavior of the A exciton in Fig. 11 with that of electronic or vibronic infrared absorption bands which were tentatively ascribed to defects involving C_I (carbon on an interstitial site),

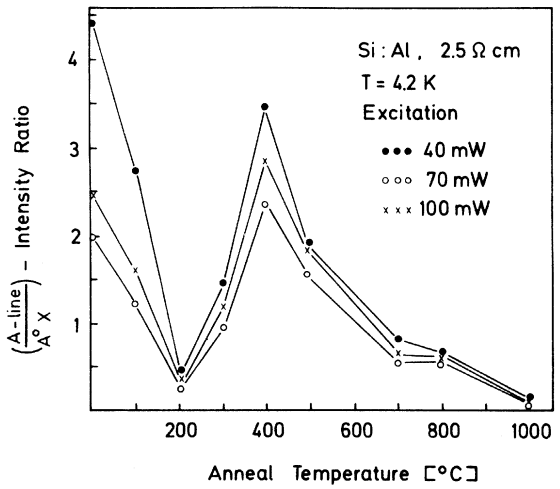

FIG. 11. Ratio of luminescence from A and A^0X bound excitons vs isochronal anneal temperature. The three sets of data points were obtained in independent experiments with laser excitation powers as indicated.

C-O associates and $Si_I + O_I$.[56,57] The number density of these defects grows on heating at ≈180 °C and disappears at temperatures between 220 and 360 °C. This annealing behavior is complimentary to that found in Fig. 11 close to 200 °C. Oxygen-related defects should not be considered in the present case since no correlation with the fluorescent intensities is apparent from Table I. Although from the present data it is premature to claim a correlation of the isoelectronic trap with carbon on a substitutional lattice site this may serve as a hypothesis for future work. Isotope shifts of the luminescence from samples containing ^{12}C and ^{14}C could give an answer as to the participation of carbon. However, even if it were proven that substitutional carbon is one trap constituent the partners are not yet known.

III. SUMMARY

This paper reports on a new exciton in silicon bound to an isoelectronic trap of axial ⟨111⟩ symmetry. The exciton has a high radiative quantum efficiency despite the large binding energy, E_{Bx} ≈ 33 meV. Combination of the basic spectroscopic data with temperature- and time-dependent measurements and with Zeeman data results in the determination of the exciton level scheme. This is made up of two low-lying levels classified by $J_z = \pm 2$ and $J_z = \pm 1$. Dipole allowed transitions from the latter state result in the strong A line, transitions from the former state corresponding to the B-exciton level become allowed when external perturbing magnetic or elastic strain fields are applied. A third broader line C originates from a higher-energy exciton level which may be composed of overlapping electron-hole $J_z = 0, \pm 1$ states. Many of the observed properties are highly reminiscent of familiar isoelectronic systems, and the closest analogy is found to exist between the present exciton states and the exciton bound to the center Li-Li-O in GaP. Current injection is reported to be a convenient tool of exciting the exciton luminescence and to study the phonon structure of the spectra. Hence, intimate knowledge of the electronic structure of the localized exciton is obtained.

In contrast, little can be said about the isoelectronic center trapping the exciton. The trap is as-grown and present in concentrations below some 10^{13} cm^{-3}, and exists in pulled crystals as well as in floating zone material. A correlation with shallow donors or acceptors could not be established. At least two atoms constitute the center, and one of these may be carbon. This is a hypothesis, and a lot of future work seems necessary to elucidate the nature of the isoelectronic trap.

ACKNOWLEDGMENTS

We are grateful to F. Köhl (Wacker Chemitronic, Burghausen) for providing a great deal of silicon crystals and for selecting specific crystals of high carbon concentration. We are also indebted to Dr. K. Graff (AEG-Telefunken, Heilbronn) and to W. Forkel for independent determinations of oxygen and carbon concentrations of the samples by ir absorption or by tunneling spectroscopy, respectively. Thanks are due to our colleagues A. Forchel and W. Kuebart for their valuable expert assistance in experiments and in technological problems. It is a pleasure to thank G. Hettich for the annealing of the samples and M. Pilkuhn for his steady and stimulating interest in the work. This investigation was supported in part by the Federal Ministry of Research and Technology (Contract No. NT 08569) and by the Deutsche Forschungsgemeinschaft (SFB 67).

[1]R. E. Dietz, D. G. Thomas, and J. J. Hopfield, Phys. Rev. Lett. 8, 391 (1962).
[2]J. J. Hopfield, D. G. Thomas, and R. T. Lynch, Phys. Rev. Lett. 17, 312 (1966).
[3]D. G. Thomas, M. Gershenzon, and J. J. Hopfield, Phys. Rev. 131, 2397 (1963).
[4]Y. Yafet and D. G. Thomas, Phys. Rev. 131, 2405 (1963).
[5]D. G. Thomas, J. J. Hopfield, and C. J. Frosch, Phys. Rev. Lett. 15, 857 (1965).
[6]D. G. Thomas and J. J. Hopfield, Phys. Rev. 150, 680 (1966).
[7]F. A. Trumbore, M. Gershenzon, and D. G. Thomas, Appl. Phys. Lett. 9, 4 (1966).
[8]B. Welber, Phys. Lett. A 29, 401 (1969).
[9]P. J. Dean and R. A. Faulkner, Phys. Rev. 185, 1064 (1969).
[10]A. Onton and T. N. Morgan, Phys. Rev. B 1, 2592 (1970).
[11]P. J. Dean, J. D. Cuthbert, and R. T. Lynch, Phys. Rev. 179, 754 (1969).
[12]A. C Aten and J. H. Haanstra, Phys. Lett. 11, 97 (1964).
[13]A. C. Aten, J. H. Haanstra, and H. de Vries, Philips Res. Rep. 20, 395 (1965).
[14]P. J. Dean, A. M. White, E. W. Williams, and M. G. Astles, Solid State Commun. 9, 1555 (1971).
[15]A. M. White, P. J. Dean, K. M. Fairhurst, W. Bardsley, and B. Day, J. Phys. C 7, L35 (1974).
[16]W. Rühle, W. Schmid, R. Meck, N. Stath, J. U. Fischbach, I. Strottner, K. W. Benz, and M. Pilkuhn, Phys. Rev. B 18, 7022 (1978).
[17]J. M. Feldman and K. M. Hergenrother, J. Appl. Phys. 42, 5563 (1971).
[18]T. N. Morgan, B. Welber, and R. N. Barghara, Phys. Rev. 166, 751 (1968).
[19]C. H. Henry, P. J. Dean, and J. D. Cuthbert, Phys. Rev. 166, 754 (1968).
[20]P. J. Dean, Phys. Rev. B 4, 2596 (1971).
[21]W. Czaja, in *Festkörperprobleme*, edited by O. Madelung (Vieweg, Braunschweig, 1971), Vol. XI, p. 65.
[22]P. J. Dean, J. Lumin. 7, 51 (1973).
[23]A. Baldereschi, J. Lumin. 7 79 (1973).
[24]G. S. Mitchard, S. A. Lyon, K. R. Elliott, and T. C. McGill, Solid State Commun. 29, 425 (1979); the P and R lines were previously reported under the labels U_2 and U_3 by M. A. Vouk and E. C. Lightowlers (see Ref. 29).
[25]E. Gmelin, *Kälte Klimatech.* 12, 531 (1976).
[26]J. Weber, W. Schmid, and R. Sauer, J. Lumin. 18/19, 93 (1979)—Proceedings of the International Conference on Luminescence, Paris, 1978.
[27]M. L. W. Thewalt, Phys. Rev. Lett. 38, 521 (1977).
[28]S. A. Lyon, D. L. Smith, and T. C. McGill, Phys. Rev. B 17, 2620 (1978).
[29]M. A. Vouk and E. C. Lightowlers, J. Lumin. 15, 357 (1977).
[30]W. Bludau, A. Onton, and W. Heinke, J. Appl. Phys. 45, 1846 (1974).
[31]K. R. Elliott, D. L. Smith, and T. C. McGill, Solid State Commun. 27, 317 (1978).
[32]E. I. Gershenzon, G. N. Gol'tsman, and A. P. Mel'nikov, Zh. Eksp. Teor. Fiz. Pis'ma Red. 14, 281 (1971) [JETP Lett. 14, 185 (1971)].
[33]E. M. Gershenzon, in *Proceedings of the Twelfth International Conference on the Physics of Semiconductors, Stuttgart* 1974, edited by M. H. Pilkuhn (Teubner, Stuttgart, 1974), p. 355.
[34]P. Norton, Phys. Rev. Lett. 37, 164 (1976).
[35]J. R. Haynes, Phys. Rev. Lett. 4, 361 (1960).
[36]K. L. Shaklee and R. E. Nahory, Phys. Rev. Lett. 24, 942 (1970).
[37]W. Schmid, Phys. Status Solidi B 84, 529 (1977).
[38]D. A. Lyon, G. C. Osbourne, D. L. Smith, and T. C. McGill, Solid State Commun. 23, 425 (1977).
[39]G. C. Osbourne and D. L. Smith, Phys. Rev. B 16, 5426 (1977).
[40]J. D. Cuthbert and D. G. Thomas, Phys. Rev. 154, 763 (1967).
[41]J. W. Morgan and T. N. Morgan, Phys. Rev. B 1, 739 (1970).
[42]G. Feher, J. C. Hensel, and E. A. Gere, Phys. Rev. Lett. 5, 309 (1960).
[43]These values were obtained from $g_{\parallel}$ and $g_{\perp}$ in Fig. 3 of Ref. 42 using the following relations: $g_{\parallel} = g_1' + \frac{1}{4} g_2'$ and $g_{\perp} = 2g_1' + 5g_2'$ which result from the diagonalization of the Hamiltonian containing strain- and magnetic field-dependent terms; see, e.g., K. Suzuki, M. Okazaki, and H. Hasegawa, J. Phys. Soc. Jpn. 19, 930 (1964).
[44]G. Feher, Phys. Rev. 114, 1219 (1959).
[45]J. M. Cherlow, R. L. Aggarwal, and B. Lax, Phys. Rev. B 7, 4547 (1973).
[46]J. Weber, thesis (Stuttgart, 1979) (unpublished); R. Sauer, Habilitationsschrift (Stuttgart, 1978) (unpublished).
[47]W. Forkel, thesis (Stuttgart, 1977) (unpublished).
[48]R. Sauer, in *Proceedings of the Twelfth International*

Conference on the Physics of Semiconductors, Stuttgart, 1974, edited by M. H. Pilkuhn (Teubner, Stuttgart, 1974), p. 42.
[49]R. Sauer, Phys. Rev. Lett. 31, 376 (1973).
[50]P. J. Dean, J. R. Haynes, and W. F. Flood, Phys. Rev. 161, 711 (1967).
[51]B. N. Brockhouse, Phys. Rev. Lett. 2, 256 (1959).
[52]D. L. Dexter, *Solid State Physics*, edited by F. Seitz and D. Turnbull (Academic, New York, 1958), Vol. 6, p. 353 (see especially p. 370); and D. L. Dexter, Phys. Rev. 101, 48 (1956).
[53]P. J. Dean, W. F. Flood, and G. Kaminsky, Phys. Rev. 163, 721 (1967).
[54]See, e.g., the review by J. W. Corbett and J. C. Bourgoin, in *Point Defects in Solids*, edited by J. H. Crawford and L. M. Slifkin (Plenum, New York and London, 1975), p. 1.
[55]J. R. Noonan, C. G. Kirkpatrick, and B. G. Streetman, Radiat. Eff. 21, 225 (1974); C. G. Kirkpatrick, J. R. Noonan, and B. G. Streetman, *ibid.* 30, 97 (1976), and references therein.
[56]A. R. Bean, R. C. Newman, and R. S. Smith, J. Phys. Chem. Solids 31, 739 (1970).
[57]Further reference is given in the review, Ref. 56; this article contains an annealing diagram on C_I- and $(Si_I + O_I)$ -related defects (Fig. 30) but the temperature scale is erroneously labeled in units of °K instead of °C.